Dynamic structure of *pharaonis* phoborhodopsin (sensory rhodopsin II) and complex with a cognate truncated transducer as revealed by site-directed ^{13}C solid-state NMR

Tadashi Arakawa[a], Kazumi Shimono[b], Satoru Yamaguchi[a], Satoru Tuzi[a], Yuki Sudo[b], Naoki Kamo[b], Hazime Saitô[a,*]

[a] *Department of Life Science, Graduate School of Science, Himeji Institute of Technology, Harima Science Garden City, Kouto 3-chome, Kamigori, Hyogo 678-1297, Japan*

[b] *Laboratory of Biophysical Chemistry, Graduate School of Pharmaceutical Sciences, Hokkaido University, Sapporo 060-0812, Japan*

Received 11 October 2002; accepted 12 December 2002

First published online 24 January 2003

Edited by Thomas L. James

Abstract **We have recorded ^{13}C nuclear magnetic resonance (NMR) spectra of [3-^{13}C]Ala, [1-^{13}C]Val-labeled *pharaonis* phoborhodopsin (*p*pR or sensory rhodopsin II) incorporated into egg PC (phosphatidylcholine) bilayer, by means of site-directed high-resolution solid-state NMR techniques. Seven ^{13}C NMR signals from transmembrane α-helices were resolved for [3-^{13}C]Ala-*p*pR at almost the same positions as those of bacteriorhodopsin (bR), except for the suppressed peaks in the loop regions in spite of the presence of at least three Ala residues. In contrast, ^{13}C NMR signals from the loops were visible from [1-^{13}C]Val-*p*pR but their peak positions of the transmembrane α-helices are not always the same between *p*pR and bR. The motional frequency of the loop regions in *p*pR was estimated as 10^5 Hz in view of the suppressed peaks from [3-^{13}C]Ala-*p*pR due to interference with proton decoupling frequency. We found that conformation and dynamics of *p*pR were appreciably altered by complex formation with a cognate truncated transducer *p*Htr II (1–159). In particular, the C-terminal α-helix protruding from the membrane surface is involved in the complex formation and subsequent fluctuation frequency is reduced by one order of magnitude.**

Key words: *Pharaonis* phoborhodopsin; Sensory rhodopsin II; Cognate transducer; Membrane protein; Conformation and dynamics; Site-directed ^{13}C solid-state NMR

1. Introduction

Halobacteria contain a family of four retinal proteins, bacteriorhodopsin (bR), halorhodopsin (hR), sensory rhodopsin I (sR I) and phoborhodopsin (pR or sensory rhodopsin II, sR II), which carry two distinct functions through common photochemical reaction. In particular, bR and hR are light-driven ion pumps transporting proton and chloride, respectively [1], while the two sensory rhodopsins are photoreceptors active for positive and negative phototaxis, respectively [2]. Here, *pharaonis* phoborhodopsin (*p*pR) is a pigment protein from *Natronobacterium pharaonis* and corresponds to pR of *Halobacterium salinarum* with 50% homology of amino acid sequence [3,4]. These two photoreceptors with proton transport ability are activated to yield signaling for phototaxis, through their plausible conformational changes, after receiving incoming light by tightly complexed to their respective cognate transducers consisting of two transmembrane helices (TM1 and TM2), Htr I and Htr II, respectively [5]. In contrast, photo-induced proton transport of *p*pR ceased by association with the transducer Htr II [6].

Three-dimensional structures of *p*pR have recently been revealed by electron crystallographic analysis of two-dimensional crystals or X-ray diffraction studies of three-dimensional crystals [7–9]. Their revealed structures showed higher degree of similarity with those of bR, with minor changes in retinal pocket and unbent retinal, reflecting their respective biological functions such as proton transport and signal transduction. In addition, transient movement of helix F in *p*pR and receptor–transducer signal transfer were analyzed by means of electron paramagnetic resonance study on spin-labeled *p*pR and Htr II and their complex [10,11]. In contrast, we have demonstrated that a site-directed solid-state ^{13}C nuclear magnetic resonance (NMR) approach provides an alternative means to delineate conformation and dynamics of ^{13}C-labeled bR as a typical membrane protein at ambient temperature, once resolved ^{13}C signals, if any, could be assigned to certain residues of interest utilizing site-directed mutants [12–14] and conformation-dependent displacement of ^{13}C chemical shifts [15,16]. This approach turned out to be especially useful as a complementary means to diffraction studies in which structural data of surfaces such as C- or N-terminals as well as loop regions are in many instances lost owing to a disordered or motionally averaged state [12–14].

In the present paper, we have recorded ^{13}C NMR spectra of [3-^{13}C]Ala, [1-^{13}C]Val-labeled *p*pR and its complex with a truncated cognate transducer *p*Htr II (1–159) reconstituted in egg PC bilayer, in order to gain insight into the dynamic features of free *p*pR and its complex with the transducer.

2. Materials and methods

[3-^{13}C]Ala, [1-^{13}C]Val-labeled *p*pR with a histidine-tag at the C-terminus expressed in *Escherichia coli* BL21 (DE3) strain was grown in the M9 medium to which ^{13}C-labeled L-Ala and L-Val were added and solubilized with 1.5% *n*-dodecyl β-D-maltoside (DM), followed by pu-

*Corresponding author. Fax: (+81)-791-58 0182.
E-mail address: saito@sci.himeji-tech.ac.jp (H. Saitô).

0014-5793/03/$22.00 © 2003 Published by Elsevier Science B.V. on behalf of the Federation of European Biochemical Societies.
doi:10.1016/S0014-5793(03)00065-6

rification with Ni-NTA resin (Qiagen) as described previously [15]. The purified protein was mixed with lipid film of egg PC (1:50 mol ratio) in which chloroform solvent was evaporated and DM as detergent was removed with Bio-Beads (SM2; Biorad) to yield *p*pR incorporated into egg PC bilayer. The reconstituted preparation was further concentrated by centrifuging and suspended in 5 mM HEPES (pH 7) buffer containing 10 mM NaCl. The truncated transducer *p*Htr II (1–159) was expressed in *E. coli* BL21 (DE3) [16]. The 1:1 mixture of *p*pR and *p*Htr II (1–159) in DM was dialyzed against distilled water. Pelleted preparations of *p*pR and its complex with the transducer were placed into a 5 mm outer diameter zirconia pencil-type rotor for magic-angle spinning after tightly sealing with glue.

^{13}C NMR spectra were recorded on a Varian CMX 400 Infinity spectrometer at ambient temperature (20°C) by cross-polarization–magic-angle spinning (CP-MAS) and dipolar decoupled–magic-angle spinning (DD-MAS). Spectral width, acquisition and contact times were 40 kHz, 50 ms, and 1 ms, respectively. Repetition times for the CP-MAS and DD-MAS spectra were 4.0 and 6.0 s, respectively. Free induction decays were acquired with data points of 2K and Fourier transform was performed as 16K after 14K points were zero-filled. ^{13}C chemical shifts were referred to tetramethylsilane (TMS) through the carboxyl ^{13}C chemical shift of glycine (176.03 ppm).

3. Results and discussion

3.1. Comparison of ^{13}C NMR spectra between ppR and bR

Fig. 1 shows the high-field region (12–20 ppm) of the ^{13}C CP-MAS (A) and DD-MAS (B) NMR spectra of [3-^{13}C]Ala-, [1-^{13}C]Val-labeled *p*pR incorporated into egg PC bilayer at ambient temperature, as compared with those of bacteriorhodopsin (bR) (C,D). The intense peak at 14.1 ppm was assigned to a lipid methyl peak from egg PC in view of its absence without *p*pR. Seven ^{13}C NMR signals were resolved for [3-^{13}C]Ala-*p*pR, which are ascribed to the transmembrane α-helices, corresponding to the peak positions of bR consisting of normal α_I helices and α_{II} helices with low frequency fluctuation [17], although ^{13}C NMR signals from the loop regions were completely suppressed in spite of the presence of three Ala residues. The spectral feature of the transmembrane helices in *p*pR is very similar to that of bR in spite of sequence homology of 27% [3], because similar amounts of Ala residues are present between the two types of proteins. In contrast, the ^{13}C CP-MAS NMR signals of [1-^{13}C]Val-*p*pR (Fig. 2A) are fully visible both from the transmembrane α-helices and loops, although their ^{13}C NMR signals are generally broadened and their peak intensities are suppressed to some extent as compared with those of bR (Fig. 2C). Notably, the two low-field peaks present for bR at 177.0 and 177.8 ppm are absent for *p*pR. The five signals resonated at the loop regions could be ascribed to five Val residues in the B–C and F–G loops, although the ^{13}C peak of Val^{118} could be also displaced upper field by 1–2 ppm to this region due to Val–Pro sequence [18]. The intense peak at 173.6 ppm of the DD-MAS NMR spectrum is undoubtedly ascribed to Val residues located at the C-terminal tail.

It is demonstrated that the ^{13}C NMR spectral profile of *p*pR is very similar between [3-^{13}C]Ala-labeled *p*pR and bR, but distinct spectral changes were noted for [1-^{13}C]Val-labeled proteins. The former arises from similar numbers of Ala residues in the respective transmembrane helices. On the contrary, the relative proportion of Val residues differs substantially among these transmembrane α-helices between them. In particular, one of the low-field peaks of bR (177.0 ppm) is ascribed to Val 213 [14] located at retinal pocket. Theoretically, ^{13}C chemical shift of the carbonyl carbon varies with both the torsion angles at the peptide unit and the manner of hydrogen bonding [19]. Therefore, the presence of the low-field peaks at 177.0 and 177.8 ppm in bR is caused by strong hydrogen bond interactions in view of the similarity in the torsion angles of the α-helix. In fact, Val 213 of bR participates in bifurcated three-center hydrogen bonds with Val 217 (with hydrogen bond length of 2.81 Å) and Gly 218 (with 2.78 Å) [20]. The corresponding Val 203 in *p*pR is hydrogen-bonded to Phe 208 alone with 2.86 Å [8].

Interestingly, ^{13}C NMR signals from the loop regions of

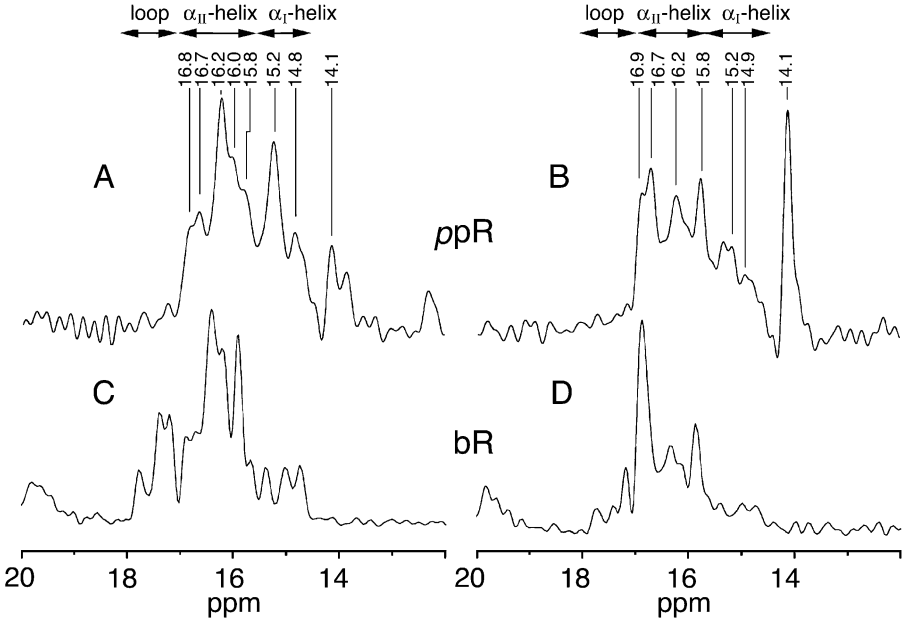

Fig. 1. ^{13}C CP-MAS (left) and DD-MAS (right) NMR spectra of [3-^{13}C]Ala, [1-^{13}C]Val-labeled *pharonis* phoborhodopsin (A,B) as compared with those of [3-^{13}C]Ala-labeled bacteriorhodopsin (C,D). ^{13}C NMR signals of the high-field region (12–20 ppm) from the [3-^{13}C]Ala-proteins alone are presented.

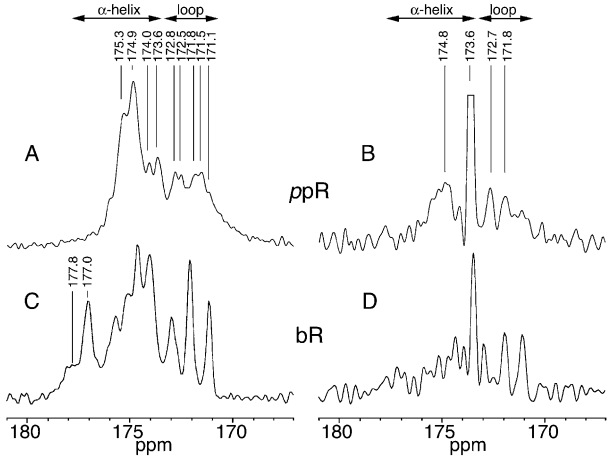

Fig. 2. ^{13}C CP-MAS (left) and DD-MAS (right) NMR spectra of [3-^{13}C]Ala, [1-^{13}C]Val-labeled *pharonis* phoborhodopsin (A,B) as compared with those of [1-^{13}C]Val-labeled bacteriorhodopsin (C,D). ^{13}C NMR signals of the low-field region (170–180 ppm) from the [1-^{13}C]Val-proteins alone are presented.

[3-^{13}C]Ala-labeled *p*pR are completely suppressed both in the CP-MAS and DD-MAS spectra (Fig. 1A,B), although ^{13}C NMR signals are fully visible for [3-^{13}C]Ala-bR [21]. Instead, the corresponding ^{13}C NMR signals of [1-^{13}C]Val-*p*pR are clearly visible (Fig. 2). The absence of the ^{13}C NMR signals of the loop region was also noted for blue membranes of wild type and D85N mutants [22,23]. In general, ^{13}C NMR signals from membrane proteins are suppressed when the fluctuation frequency in the order of 10^4 or 10^5 H_2 interferes with the frequency of the magic-angle spinning or proton decoupling, respectively [13,14,24–27]. In this connection, we have recently demonstrated that the dynamic structure of bR is substantially modified when 2D crystals of a hexagonally packed lattice were disrupted or distorted by modified helix–helix and helix–lipid interactions as in W80L and W12L mutants [28]. As a result, broadened ^{13}C NMR signals were visible from [3-^{13}C]Ala-labeled proteins but corresponding signals from [1-^{13}C]Val-labeled proteins were completely suppressed. This is because the correlation times of motional fluctuations in W80L or W12L mutants were substantially changed for the transmembrane α-helices and loops from 10^{-2} to 10^{-4} s and by one order of magnitude from 10^{-4} to 10^{-5} s, respectively [28].

In this connection, it is rather surprising to see such well resolved ^{13}C NMR signals from [3-^{13}C]Ala-labeled *p*pR and also from the [1-^{13}C]Val-labeled probe. This kind of favored situation for ^{13}C NMR observation may arise from escape from the specific time scale of 10^{-4} or 10^{-5} s owing to the use of egg PC, rather than a possibility of a 2D crystalline lattice.

3.2. *Conformational change in* p*pR due to complex formation with* p*Htr II (1–159)*

Fig. 3 illustrates the ^{13}C CP-MAS NMR signals of the low-field Val carbonyl group (A) and high-field Ala methyl (B) regions of *p*pR complexed with *p*Htr II (1–159) together with the corresponding DD-MAS spectra (C,D) superimposed upon the corresponding spectra of free *p*pR (dotted trace). The following two kinds of spectral changes are noteworthy: First, all the ^{13}C NMR signals from [3-^{13}C]Ala-labeled *p*pR (Fig. 3B) gave rise to five well-resolved peaks upon the complex formation. Second, the peak intensities of the transmembrane α-helices of [1-^{13}C]Val-labeled *p*pR are appreciably suppressed in the CP-MAS spectrum as compared with those of free *p*pR, leaving no spectral change for the loop region. The intense peak at 173.5 ppm mainly arising from Val residues located in the C-terminal tail is significantly suppressed for the complex (Fig. 3C). This is obviously caused by the presence of a dynamics change in *p*pR including the C-terminal tail due to the complex formation. Such a change is most distinct for the C-terminal α-helix (resonated at 15.9 ppm) protruding from the membrane surface (Fig. 3B) [12–14,26,27].

The altered spectral pattern to six signals in *p*pR complexed with the transducer is evident both for the CP-MAS and DD-MAS NMR spectra (Fig. 3B,D), in addition to the data of the C-terminal α-helix from the CP-MAS spectrum. In particular, the spectral resolution of ^{13}C NMR signals was appreciably improved as viewed from [3-^{13}C]Ala-labeled *p*pR, but corresponding ^{13}C NMR signals from [1-^{13}C]Val-ppR were broadened due to a dynamics change caused by the complex formation. In particular, low frequency motions in the transmembrane α-helices of *p*pR were reduced by approximately one order of magnitude with correlation time changes from the order of 10^{-5} to 10^{-4} s. The presence of this sort of dynamics change is consistent with a view of the proposed complex consisting of 2:2 stoichiometry [11,16].

The following two factors have been proposed as a cause of stabilization of the *p*pR–transducer complex: Royant et al. proposed the presence of a unique patch of charged and polar residues at the cytoplasmic ends of helices F and G [9], while Luecke et al. and Sudo et al. proposed the importance of Tyr 199 for mutual interaction [8,29]. Here, we found that the C-terminal α-helix in *p*pR participates in the stabilization of the complex formation as manifested from its intensity change in the CP-MAS NMR spectrum: the increased peak intensity of *p*pR at 15.9 ppm is caused by efficient magnetization owing to the immobilized C-terminal α-helix protruding from the membrane surface as a result of the complex formation with the cognate transducer. This finding indicates a possibility that mutual interactions among the extended TM1 and TM2

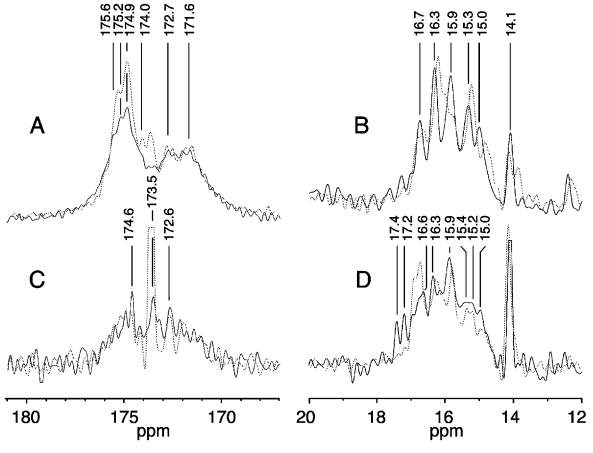

Fig. 3. ^{13}C CP-MAS (upper traces) and DD-MAS (lower traces) NMR spectra of [3-^{13}C]Ala, [1-^{13}C]Val-labeled *pharonis* phoborhodopsin complexed with *p*Htr II (1–159) (solid traces) superimposed upon those without the transducer (dotted traces). Note that the horizontal scales for the high- and low-field regions are not the same.

helices beyond the surface and the C-terminal α-helix play an important role for stabilization of the complex. This possibility may be examined by ^{13}C NMR study on ^{13}C-labeled *p*Htr II (1–159). The C-terminal α-helix itself is present even for the free *p*pR as viewed from the ^{13}C DD-MAS NMR spectrum (Fig. 1B). In bR, we have recently proposed that the C-terminal α-helix complexed with A–B, C–D or E–F loops through salt bridges or metal-ion-mediated interactions tends to prevent unnecessary fluctuations of the B and F ends of the transmembrane α-helices for efficient proton uptake during photocycle (perturbed or 'capped' form), in contrast to an unperturbed helix achieved at low temperature of M-like state of D85N (unperturbed or 'open' form) [30]. This view is consistent with the previously published data of proton binding cluster which plays an essential role to regulate the proton uptake from the cytoplasmic side [31]. In this connection, it may be assumed that the presence of the perturbed C-terminal α-helix corresponds to the function of *p*pR as proton transport, while the unperturbed C-terminal α-helix corresponds to the function of the signaling as a result of the complex formation with the transducer.

Acknowledgements: This work has been supported, in part, by a Grant-in-Aid for Scientific Research (KAKENHI) (14580629) from the MEXT, Japan.

References

[1] Lanyi, J.K. (1999) J. Struct. Biol. 124, 164–178.
[2] Hoff, W.D., Jung, K.-W. and Spudich, J.L. (1997) Annu. Rev. Biophys. Biomol. Struct. 26, 223–258.
[3] Seidel, R., Scharf, B., Gautel, M., Kleine, K., Oesterhelt, D. and Engelhard, M. (1995) Proc. Natl. Acad. Sci. USA 92, 3036–3040.
[4] Kamo, N., Shimono, K., Iwamoto, M. and Sudo, Y. (2001) Biochemistry (Moscow) 66, 1277–1282.
[5] Zhang, X.-N., Zhu, J. and Spudich, J.L. (1999) Proc. Natl. Acad. Sci. USA 96, 857–862.
[6] Sudo, Y., Iwamoto, M., Shimono, K., Sumi, M. and Kamo, N. (2001) Biophys. J. 80, 916–922.
[7] Kunji, E.R., Spudich, E.N., Grissharmer, R., Henderson, R. and Spudich, J.L. (2001) J. Mol. Biol. 308, 279–293.
[8] Luecke, H., Schobert, B., Lanyi, J.K., Spudich, E.N. and Spudich, J.L. (2001) Science 293, 1499–1503.
[9] Royant, A., Nollert, P., Edman, K., Neutze, R., Landau, E.M. and Pebay-Peyroula, E. (2001) Proc. Natl. Acad. Sci. USA 98, 10131–10136.
[10] Wegener, A.-A., Chizhov, I., Engelhard, M. and Steihoff, H.-J. (2000) J. Mol. Biol. 301, 881–891.
[11] Wegener, A.-A., Klare, J.P., Engelhard, M. and Steihoff, H.-J. (2001) EMBO J. 20, 5312–5319.
[12] Saitô, H., Tuzi, S. and Naito, A. (1998) Annu. Rep. NMR Spectrosc. 36, 79–121.
[13] Saitô, H., Tuzi, S., Yamaguchi, S., Tanio, M. and Naito, A. (2000) Biochim. Biophys. Acta 1460, 39–48.
[14] Saitô, H., Tuzi, S., Tanio, M. and Naito, A. (2002) Annu. Rep. NMR Spectrosc. 47, 39–108.
[15] Kandori, H., Shimono, K., Sudo, Y., Iwamoto, M., Shichida, Y. and Kamo, N. (2001) Biochemistry 40, 9238–9246.
[16] Sudo, Y., Iwamoto, M., Shimono, K. and Kamo, N. (2001) Photochem. Photobiol. 74, 489–494.
[17] Kimura, S., Naito, A., Tuzi, S. and Saitô, H. (2001) Biopolymers 58, 78–88.
[18] Wissshart, D.S., Sykes, B.D. and Richards, F.M. (1991) J. Mol. Biol. 222, 311–333.
[19] Ando, I., Saitô, H., Tabeta, R. and Shoji, A. (1984) Macromolecules 17, 457–461.
[20] Luecke, H., Schobert, B., Richter, H.T., Cartailer, J.P. and Lanyi, J.K. (1999) J. Mol. Biol. 291, 899–911.
[21] Tuzi, S., Naito, A. and Saitô, H. (1994) Biochemistry 33, 15046–15052.
[22] Tuzi, S., Yamaguchi, S., Tanio, M., Konishi, H., Inoue, S., Naito, A., Needleman, R., Lanyi, J.K. and Saitô, H. (1999) Biophys. J. 76, 1523–1531.
[23] Tanio, M., Tuzi, S., Yamaguchi, S., Kawaminami, R., Naito, A., Needleman, R., Lanyi, J.K. and Saitô, H. (1999) Biophys. J. 77, 1577–1584.
[24] Rothwell, W.T. and Waugh, J.S. (1981) J. Chem. Phys. 75, 2721–2732.
[25] Suwelack, D., Rothwell, W.P. and Waugh, J.S. (1980) J. Chem. Phys. 73, 2559–2569.
[26] Yamaguchi, S., Tuzi, S., Tanio, M., Naito, A., Lanyi, J.K., Neeleman, R. and Saitô, H. (2000) J. Biochem. 127, 861–869.
[27] Yamaguchi, S., Tuzi, S., Yonebayashi, K., Naito, A., Neeleman, R., Lanyi, J.K. and Saitô, H. (2001) J. Biochem. 129, 373–382.
[28] Saitô, H., Tuchida, T., Ogawa, K., Arakawa, T., Yamaguchi, S. and Tuzi, S. (2002) Biochim. Biophys. Acta 1565, 97–106.
[29] Sudo, Y., Iwamoto, M., Shimono, K. and Kamo, N. (2002) Biophys. J. 83, 427–432.
[30] Yonebayashi, K., Yamaguchi, S., Tuzi, S. and Saitô, H. (2002) Eur. Biophys. J., in press.
[31] Checover, S., Marantz, Y., Nachliel, E., Gutman, M., Pfeffer, M., Tittor, J., Oesterhelt, D. and Dencher, N.A. (2001) Biochemistry 40, 4281–4292.